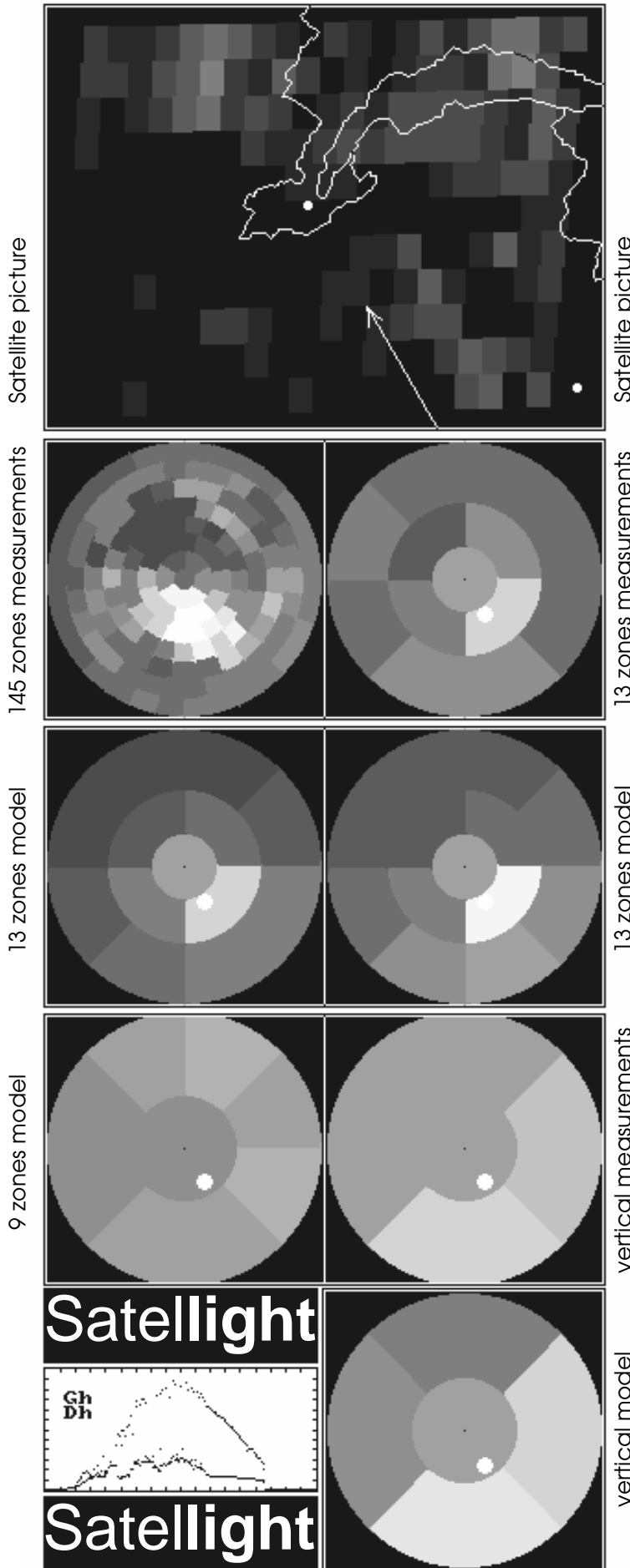


**Satellite**light

Commission of the European Communities

# Sky luminance distribution from Meteosat images



Working paper  
Pierre Ineichen  
3<sup>rd</sup> Satellite meeting  
Les Marécottes  
January 16-17, 1997

## Introduction

This document describes the path I followed to develop a model for the evaluation of the sky luminance distribution on the basis of meteosat information.

Considering the available data, there are two possible methods: the *single pixel* and the *multiple pixels* as input data. The first method will provide a model that cannot take into account the cloud distribution in the sky vault and the output data will therefore be symmetrical to the sun azimuth. The multiple pixel method, even taking into account the clouds' position, needs higher resolution input data and IR data to evaluate the altitude of the clouds; it gives bad results.

I first made the model versus measurements tests for the heliosat models with the Genave's data. The results induced discussions, and I needed a zenith luminance model, I then decided to derive my own models and to base all my work on them.

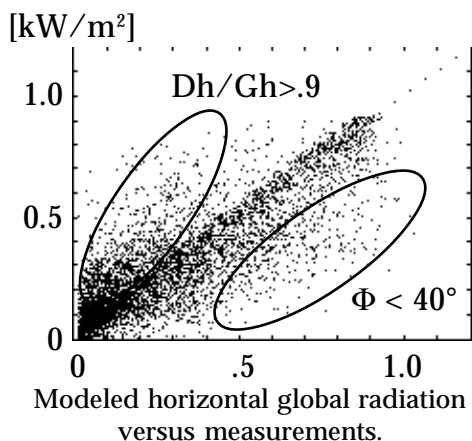
## Heliosat models.

The validation of the different heliosat model with the data from Geneva gives the following results:

Model	v2a	v2b	v2c	v2d	v3	
global 301 [W/m <sup>2</sup> ]	1%	20%	13%	5%	19%	MBD
	34%	35%	35%	35%	36%	SD
	34%	41%	37%	35%	41%	RMSD
diffuse 141 [W/m <sup>2</sup> ]	27%	22%	15%	16%	20%	MBD
	48%	44%	42%	44%	46%	SD
	55%	49%	45%	47%	50%	RMSD

MBD: mean bias difference, SD: standard deviation, RMSD: root mean square difference

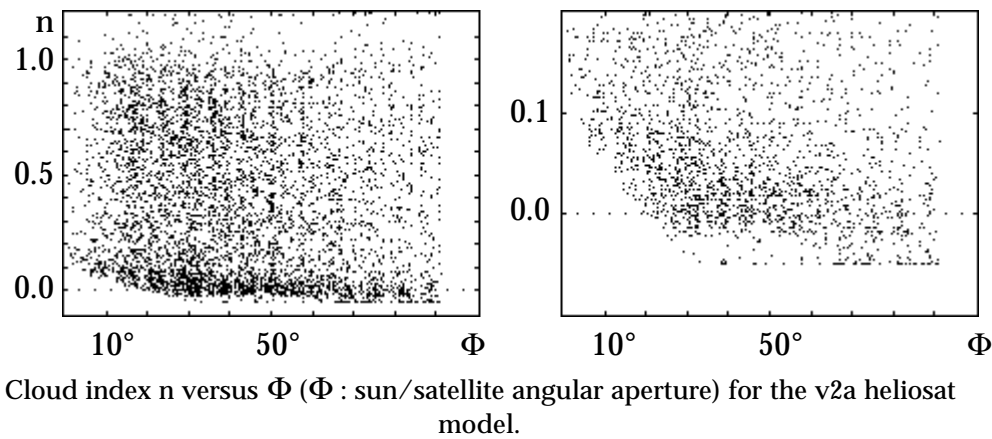
The v2b, v2c and v3 versions show a very high overestimation for June-July-august (MBD = 36% of the yearly average and 25% of the summer average) and are highly sun height (or sun/satellite angle) dependent (cf. appendix, Figure 1). Version 2d is slightly better, but shows also a summer overestimation, version 2a gives the best results.



In a previous working paper, I pointed out that the lower right points in the opposite scatter plot are representative of situations where the angular distance ( $\Phi$ ) between the sun direction and the satellite is lower than  $40^\circ$ .

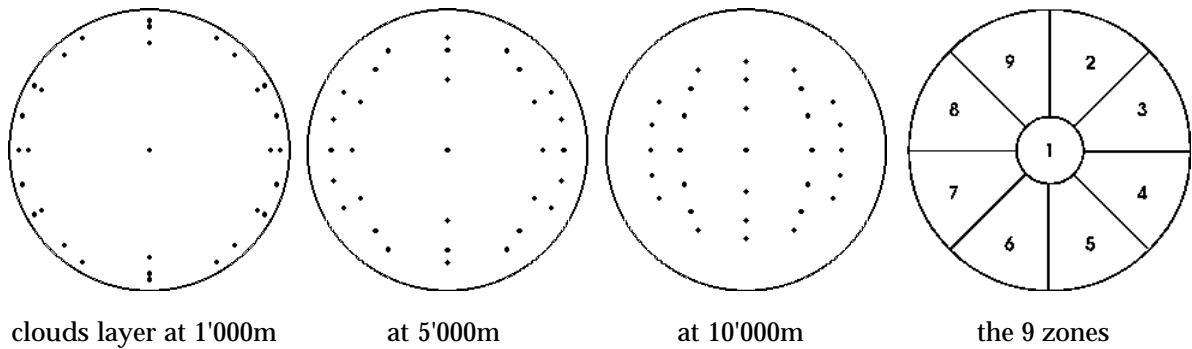
In order to explain this underestimation, I represented in the following figures the derived cloud index versus the sun/satellite angle  $\Phi$  with two different scales. It seems from these figures that there is a saturation at  $n = -0.05$  for  $\Phi$  higher than  $30^\circ$  (the figures are for the v2a model; for the v3 model, this saturation begins at  $40^\circ$ ). The conclusion could be that the albedo has to be

evaluated with more precision, particularly on a monthly basis instead of a unique yearly value (Hammer, 1996).

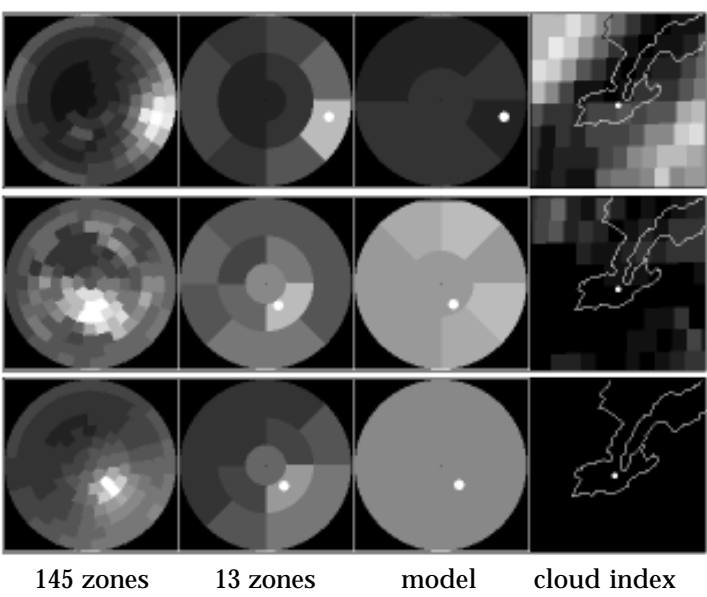


**Luminance distribution, multiple pixel model.**

The sky luminance measurements are done in 145 different angular directions, and are average values of the sky luminance in a solid angle of  $10^\circ$ . If one consider a cloud level at different



Position of the pixels in the sky vault for different cloud layers' altitude and description of the 9 zones used to derive the luminance distribution model from multiple pixel.



Luminance measurements in 145 and 13 zones, the corresponding values obtained with the multiple pixels model and the cloud index

altitudes and a 7x5 pixels region, as shown in the figure, the "resolution" for the sky luminance distribution cannot be higher than the 9 zones described in the figure. The model gives a luminance value for each of the 9 zones, evaluated on the basis of the cloud index.

The luminances obtained with such a model are not good. Indeed, the evaluated values are representative of a "diffuse" luminance, and do not take into account the influence of the sun (circumsolar diffuse). Moreover, the altitude of the clouds' layer is difficult to evaluate with enough precision to know what pixels will be involved in a defined sky region.

To better evaluate the diffusion processes involved in the sky luminance distribution, one need to know the diffuse/direct ratio of the incoming radiation. This is the other part of the project.

I decided then to use an existing luminance distribution model, the modified CIE model, and to derive the input parameters from a single pixel.

***Luminance distribution, single pixel method.***

The input parameters for the modified CIE model are the following:

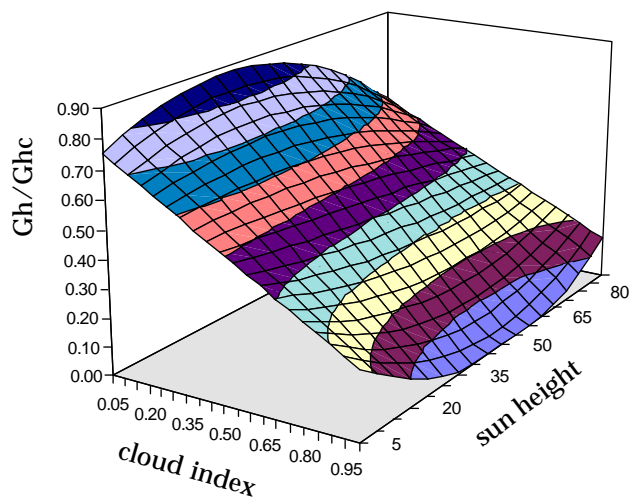
- beam and diffuse radiation to derive the sky brightness and sky clearness,
- either the zenith luminance to obtain absolute luminances, or the diffuse illuminance to normalise the relative luminances.

To evaluate the luminance, I derived my own models for the global horizontal radiation, diffuse horizontal radiation and zenith luminance. The 3 models are based on version 3 raw cloud indices and the Ineichen clear sky model (Ineichen, 1983). They are all based on the cloud index and the sun height.

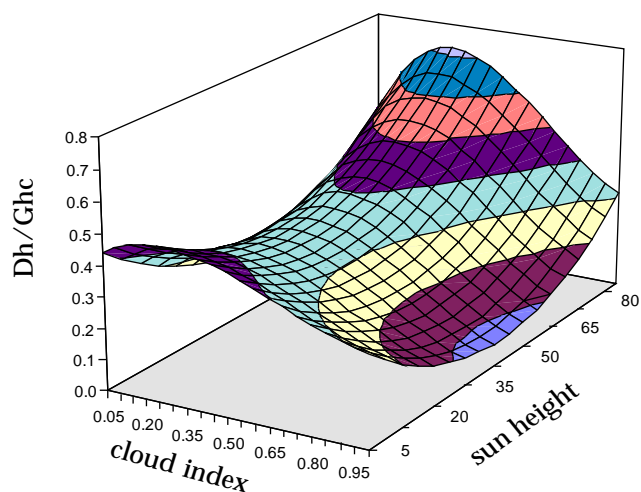
I will use a luminous efficacy model to derive the diffuse illuminance.

***Global radiation derivation.***

The study of the parameter dependance of the heliosat models shows that the global radiation is depending on the sun height (or the sun/satellite angle). The model is a regression on the cloud index and the sun height; it has a negligible bias (-1%), and a 37% RMSD (average global: 301 [W/m<sup>2</sup>]). It's variation with these two input parameters is given in the opposite figure. The cloud index dependance is linear and the sun height dependance is quadratic.



Global derivation model



Diffuse derivation model

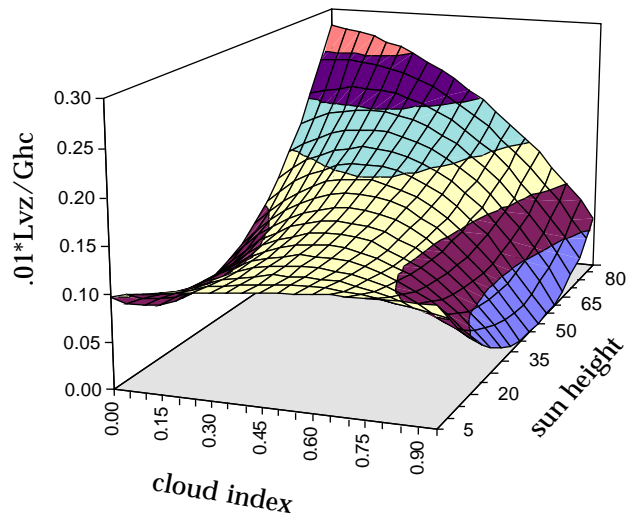
Figure 2 in the appendix gives the variation of the model for each parameter and Figure 5 (appendix) is the result of a parameter dependance study. The parameters that could improve the model seem to be the water vapour content of the atmosphere (cf. heliosat v4) and  $\delta nb$ , but this dependance has to be confirmed on other data.

***Diffuse radiation model.***

The same study can be done for the diffuse radiation using the same input parameters. The model representation is given in the opposite figure. As for the global radiation, the other figures (3 & 5) are given in appendix. The diffuse is evaluated with a slight negative bias (4%) and a 44% RMSD (average diffuse 141 [W/m<sup>2</sup>]).

### *Zenith luminance model*

I used the same method to derive the zenith luminance Lvz from the meteosat pixel. In this case, the dispersion is higher due to the shift in the measurement time between the pixel and the luminance scan. I normalised the luminance with the same clear sky model. In this case, the bias is -6% with a root mean square difference of 53% (average Lvz : 4800 [cd/m<sup>2</sup>]). The parameter dependance study, given in the appendix (Figure 4 & 5), shows no particular trend that can improve the model.



Zenith luminance derivation model

### *Diffuse illuminance*

To derive the diffuse illuminance, I will use the diffuse luminous efficacy model described in (Perez, 1990). This model, applied on the Geneva's data set (15 min. instantaneous data), gives a negligible bias and a root mean square difference of 9%.

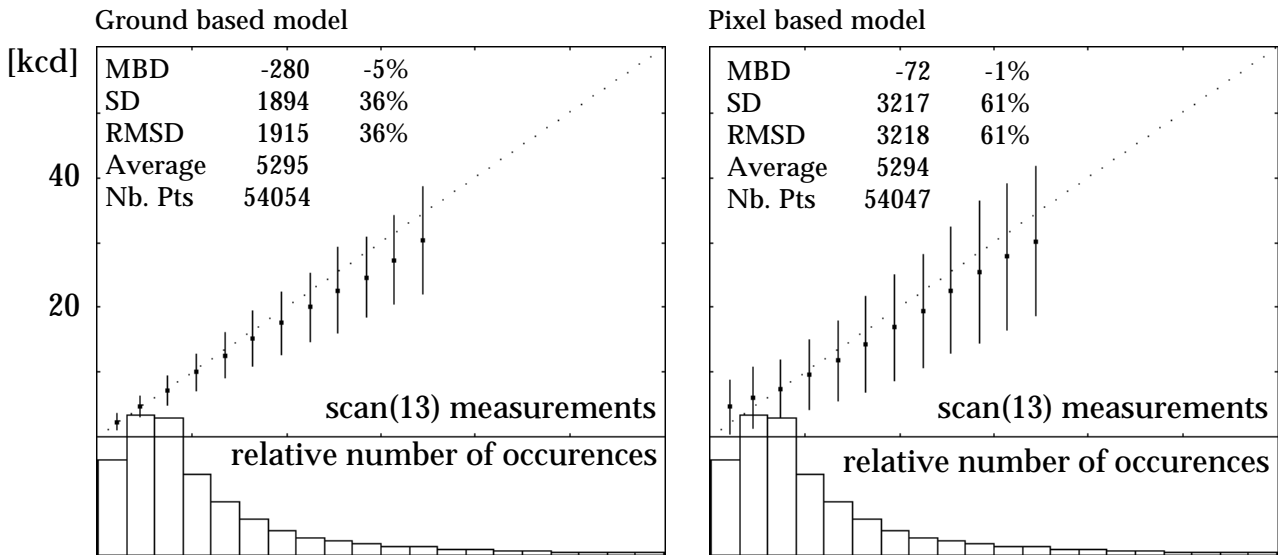
### *Luminance distribution model*

In a previous working paper, I concluded that the modified CIE model gives the best results on a 13 zones' sky (Ineichen, 1996). This model was developed by Matsuzawa (Matsuura, 1990) and is a combination of the three CIE standard skies: clear, intermediate and overcast. Perez slightly modified this model to take into account the high turbid intermediate skies. The governing parameters are the sky clearness and the sky brightness.

Using the above modeled quantities, I will quantify the precision of this sky luminance distribution model on a 13 zones' sky and on the four vertical planes.

### *Luminance distribution for a 13 zones' sky.*

The first evaluation was to apply the model on the ground based measurements and compare the modeled luminances with the measurements. This gives the "intrinsic" precision of the model. I then applied the single pixel based model to obtain absolute luminances (with Lvz model as input) and relative luminances. These relative luminances have to be normalised with the horizontal diffuse illuminance (the modeled luminances are integrated to obtain a horizontal diffuse illuminance that is normalised with the modeled diffuse illuminance). The results are presented in the following figures. One can point out that an underestimation for high values of luminance is present on both figures: it is a problem of the model itself. The overestimation for low luminances values is due to the global and diffuse models. In fact, the same trend is present for the 3 above described models (see appendix,



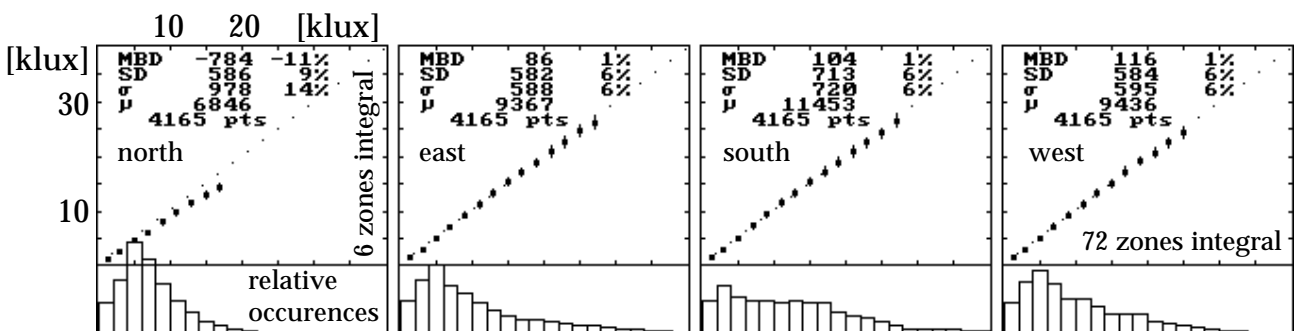
Modeled-measured luminance comparison for the CIE model based on ground inputs and pixel inputs. The luminances are normalised with Dvh (respectively Dvhm)..

figure 5). The modeled/measured graphs for each zone separately are given in Figures 6 & 7 in the appendix and they show clearly that the model overestimates in the south direction and underestimates in the north direction; the interregions (east-west) have no bias. The above figures represent relative (Dvh normalised) values of luminance. If one compares the absolute luminance with the measured luminance, the bias rises to 13%, and the RMSD to 70% (one can observe the effect on each zone separately). A parameter dependance is given on Figure 8.

The pix2lum model (modified CIE luminance distribution model, normalised with a modeled diffuse illuminance and based on modeled global and diffuse irradiances) will be used to evaluate the vertical illuminances.

*Vertical illuminances as integrals of the luminance over the sky vault.*

In order to validate the method, I compared in a first step the integrals over 145 zones with the integrals over 13 zones, for the horizontal plane and for the four vertical planes. In previous studies, I obtained a good agreement on the horizontal comparisons with the PRC Krochmann sky scanner (Ineichen, 1993, June 1996). This is confirmed with the 1994-95 data set used in this study. Concerning the vertical planes, the graphs show an underestimation of the scan integral on the north plane (11%) and a good agreement on the three other planes:



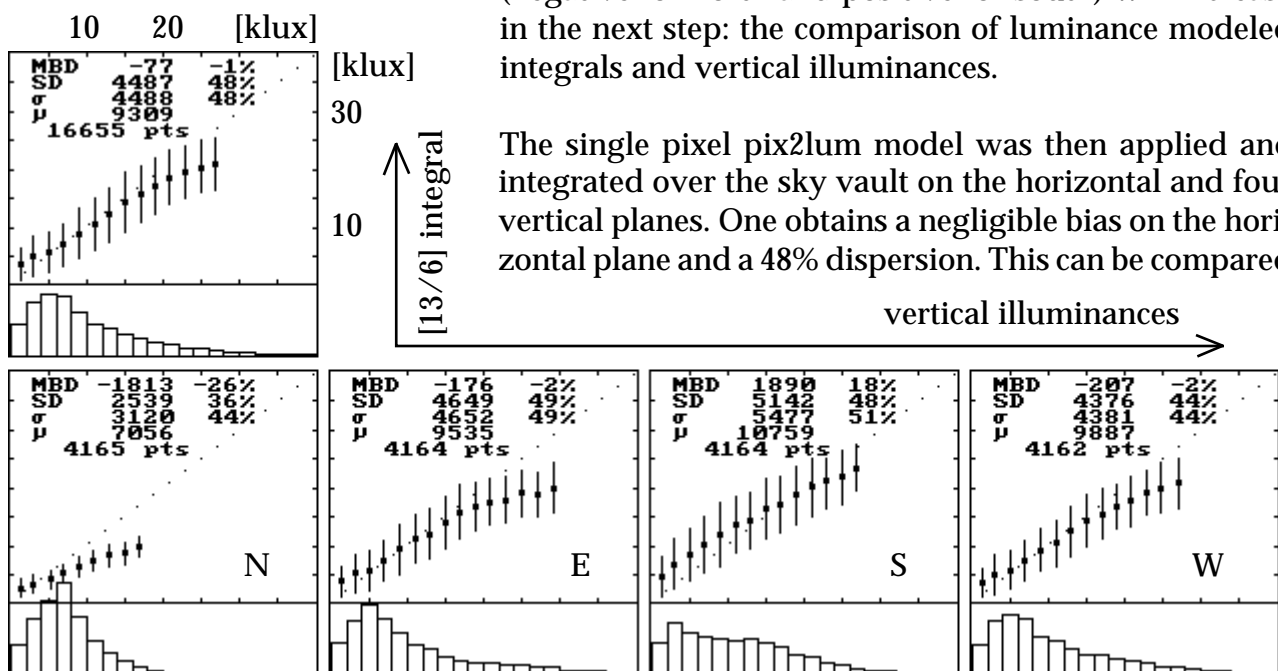
Integral over 6 zones versus integral over 72 zone for the four vertical planes (cf. Figure 9, appendix)

I then compared the 6/13 zones integrals with the horizontal and four vertical illuminances. The negative bias in the north direction increases, while a positive bias appears in the south direction. These systematic biases confirm the previous test (Ineichen, June 1996, Fig 1) where the bias was negative for bright skies with no sun and positive for clear skies with sun. It is important to note that these trends will persist in all further comparisons. The results are the following:

	Plane	horizontal	north	east	south	west
	Nb. Pts	16'660	4'165	4'165	4'165	4'165
	Average [lux]	9276	6846	9367	11453	9436
13/6 zones meas. versus 145/72 zones meas.	MBD	-1%	-11%	1%	1%	1%
	SD	8%	9%	6%	6%	6%
	RMSD	8%	14%	6%	6%	6%
13/6 zones meas. versus meas. illuminances	MBD	-2%	-14%	-1%	7%	-3%
	SD	19%	16%	16%	18%	19%
	RMSD	19%	21%	16%	19%	20%

The corresponding figures are given in the appendix (Figure 10).

These results show that one cannot expect a better precision than 20% with this method. Taking into account the pix2lum model previous results (Figure 7, appendix), the biases (negative for north and positive for south) will increase in the next step: the comparison of luminance modeled integrals and vertical illuminances.



to the bias and precision of the diffuse irradiance model (-4% and 44% respectively); it is satisfying and shows that even going through a complex modelisation, the bias and precision remains in the same order. Concerning the vertical north and south biases (MBD) and precision (RMSD) they are twice the values obtained with measurements (scan integrals versus illuminances). One can also point out that one find again the Gh, Dh and Lvz trends: an overestimation for low values and an underestimation for high values.

If one apply the modified CIE model with ground based measurements as input, one obtains the results given in Figure 11 (appendix) and summarised in the following table, last

section:

13/6 zones	Plane	horizontal	north	east	south	west
versus meas. illuminances	Nb. Pts	16'660	4'165	4'165	4'165	4'165
	Average [lux]	9276	6846	9367	11453	9436
measurements	MBD	-2%	-14%	-1%	7%	-3%
	SD	19%	16%	16%	18%	19%
	RMSD	19%	21%	16%	19%	20%
pix2lum	MBD	-1%	-26%	-2%	18%	-2%
	SD	48%	36%	49%	48%	44%
	RMSD	48%	44%	49%	51%	44%
ground based CIE	MBD	-8%	-18%	-8%	0%	-8%
	SD	25%	19%	25%	24%	25%
	RMSD	26%	27%	26%	24%	27%

This table shows also the previous results for comparison purpose: it seems that half of the biases and the dispersions are introduced by the geometric integration, and the other half by the pixel model.

### **Conclusion.**

The aim of this study is to provide a sky luminance distribution model on the basis of the meteosat pixel information. This model has to provide a better description of the daylight directionality than a vertical illuminance model. The following results were obtained:

- the five heliosat models to retrieve the cloud index from the pixel information and to evaluate the global irradiance were tested with one year data from Geneva. The results are not very satisfying, the evaluation of the albedo has to be improved. The best model is the v2a, with a negligible bias and a 34% precision,
- three models were developed on the Geneva data set to provide the basic radiation and luminance parameters. The biases are negligible and the precision are respectively for the global, diffuse radiation and the zenith luminance 37%, 43% and 53%,
- the use of the modified CIE model with the above quantities as input parameters gives a negligible bias and a dispersion of 61% for any direction in the sky vault. The model overestimates the luminance in a south direction and underestimates in the north direction. One can partly attributes these results to the intrinsic properties of the CIE model,
- when integrating the luminance distribution over the sky vault in the four vertical directions, one obtains illuminance with a bias of 1800 [lux] (negative in the north direction and positive in the south direction) with a precision of 45% to 50%. Half of these bias and dispersion are due to the integration process.

All the presented results were obtained on the data set from Geneva and for sun heights higher than 5°. They cannot be generalised for other latitudes without doing other comparisons: for a lower latitude, the circumsolar diffuse radiation will influence the zenith luminance, and for a higher latitude, the low solar altitude angles will influence the low boundary of the models.

## **References**

A. Hammer. *Global and Diffuse Radiation from Meteosat Images - an Overview about Methods for Data Derivation*. Carls von Ossietzky University, Oldenburg. Nov. 1996

P. Ineichen. *Quatre années de mesure d'ensoleillement à Genève*. Rapport de Thèse. Université de Genève. 1983.

P. Ineichen, B. Molineaux. *Characterisation and Comparison of two Sky Scanners: PRC Krochmann & EKO Instruments*. IEA Task XVII expert meeting, Geneva, Switzerland, August 1993.

P. Ineichen. *Use of Meteosat data to produce sky luminance maps*. Working paper, University of Geneva. June 1996.

P. Ineichen. *Notes on Heliosat v2a, v2b and v3: Comparison with Geneva's data*. Working paper, University of Geneva. October 1996.

R. Perez, P. Ineichen, R. Seals, J. Michalsky, R. Stewart. *Modeling Daylight Availability and Irradiance Components from Direct and Global Irradiance*. Solar Energy, Vol. 44, N° 5, pp271-289. 1990.

R. Perez, P. Ineichen, E. Maxwell, R. Seals, A. Zelenka. *Dynamic Global-to-Direct Irradiance Conversion Models*. Ashrae Transactions, V. 92, pp 3578-3593, 1992

R. Perez, J. Michalsky, R. Seals. *Modeling Sky Luminance Angular Distribution for Real Sky Conditions. Experimental Evaluation of Existing Algorithms*. Journal of the Illumination Engineering Soc. J. Vol. 21,2 pp 84-92. 1992.

K. Matsuura, T. Iwata. *A Model of Daylight Source for the Daylight Illuminance Calculations on all Weather Conditions*. CIE Daylighting Conference, Moscow. 1990

# ***Appendix***

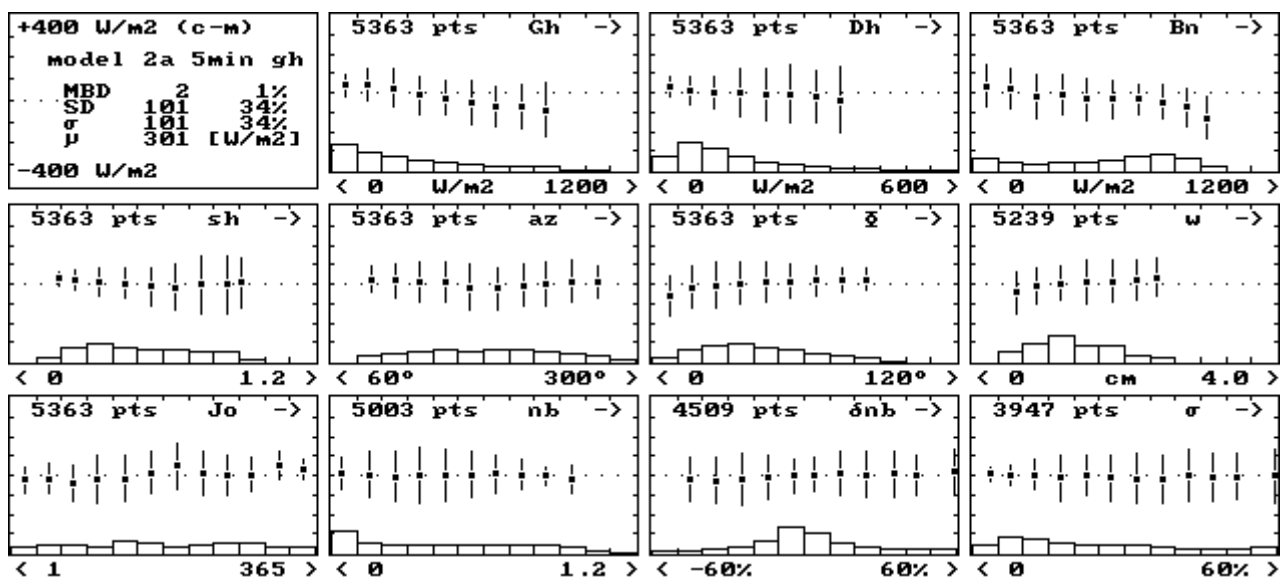
**Figure 1**

Residue of the heliosat v2a, v2b, v2c, v2d and v3 model, for the global radiation, station of Geneva and all weather conditions, versus different parameters.

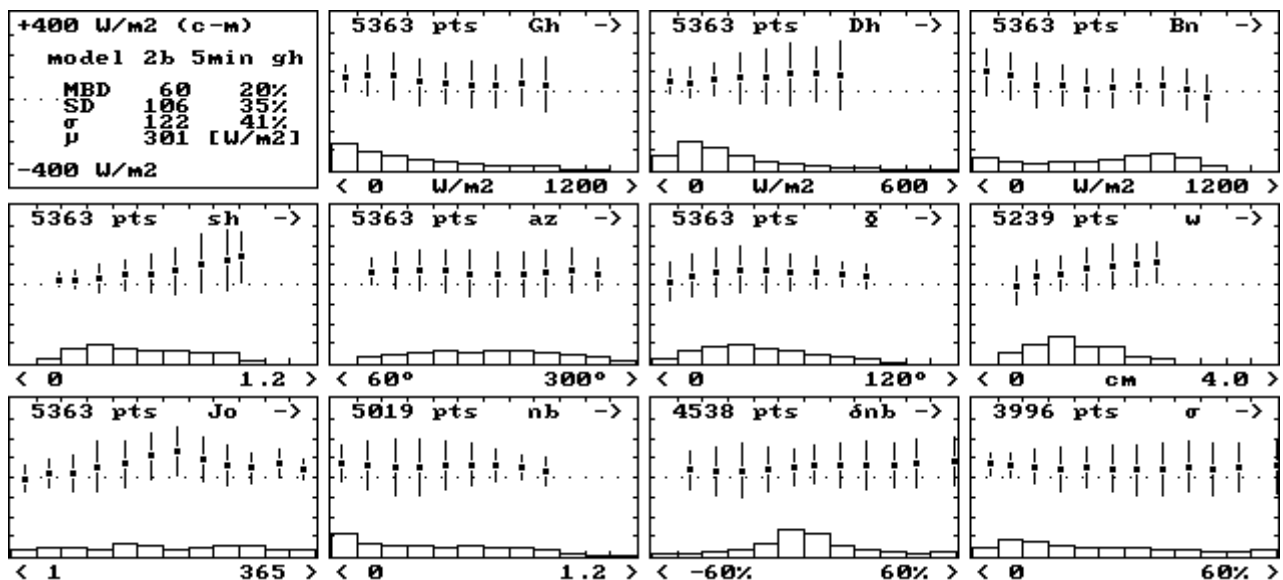
The abscissa scale is divided in bins. For each bin, the mean value is given (point) and is surrounded by  $\pm$  one standard deviation (line). The bar chart at the bottom of each dependence represents the occurrence frequency for each bin in percent of the total number of occurrences. The scale is 20% per graduation.

Gh	horizontal global	sh	sun height sine	Jo	day of the year
Dh	horizontal diffuse	az	sun azimuth	nb	nebulosity index
Bn	normal beam	$\Phi$	sun/satellite angle	$\delta nb$	nb variation (1 pix/15pix)
		w	water vapor	$\sigma$	rmsd (1 pix/15pix)

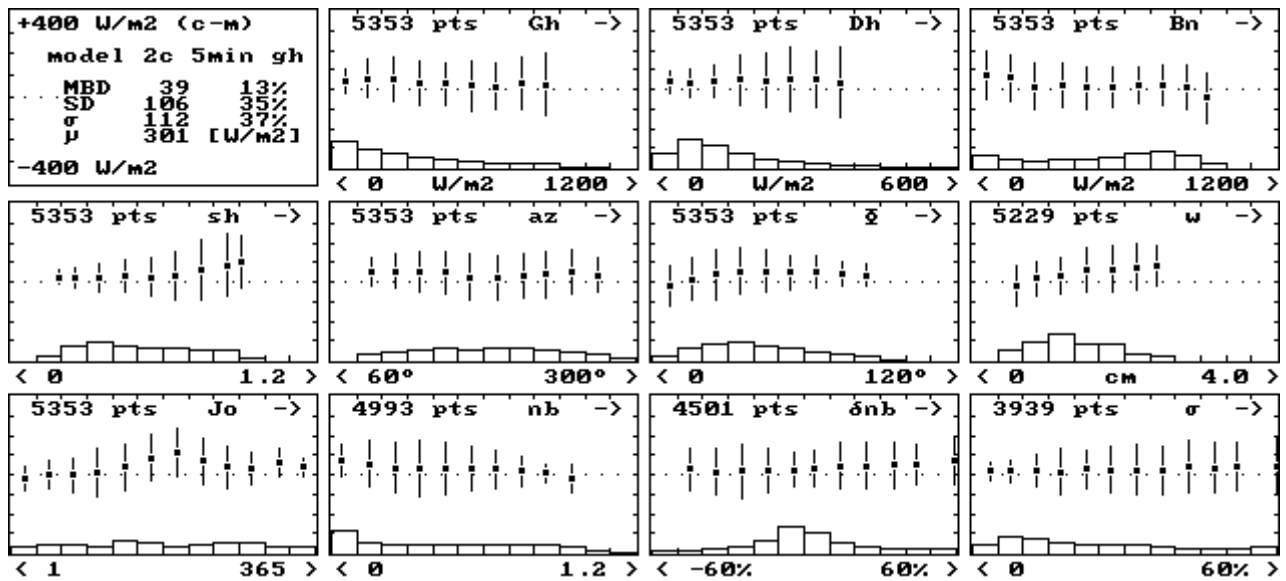
Heliosat v2a model



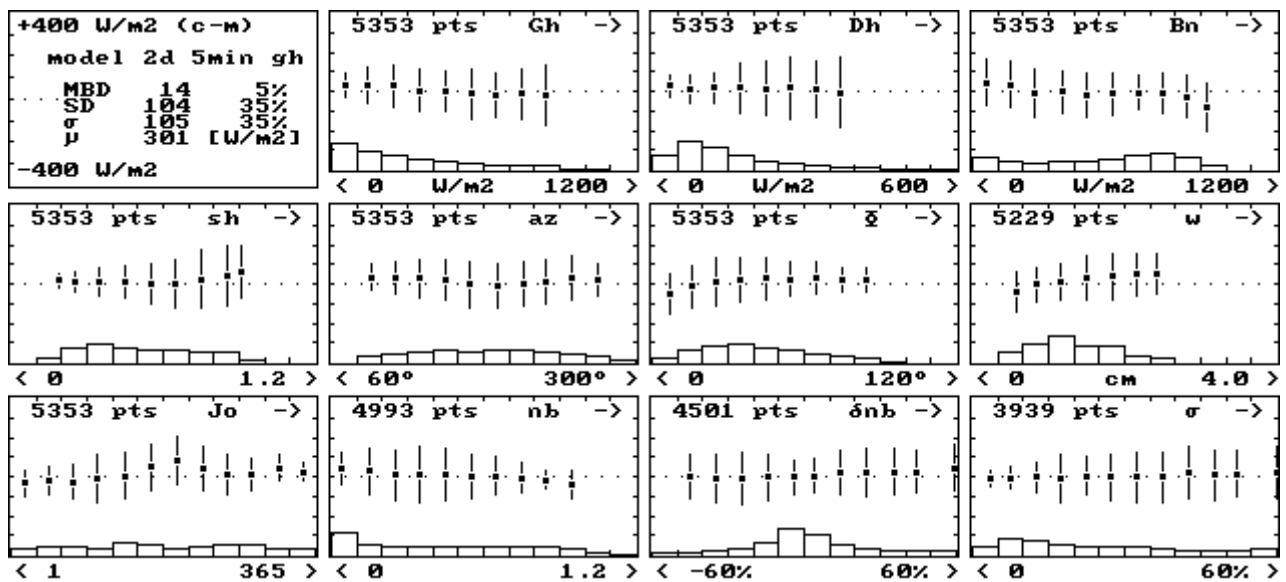
Heliosat v2b model



### Heliosat v2c model



### Heliosat v2d model



### Heliosat v3 model

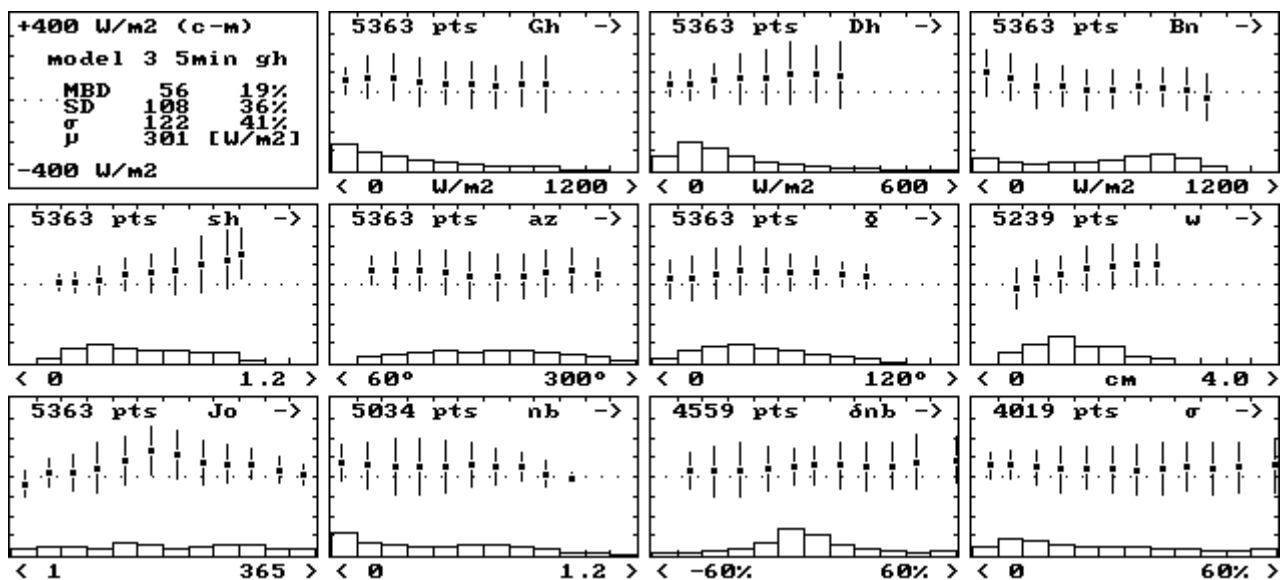


**Figure 2**

Global radiation model derivation.

The second to 6th graphs represent the normalised global versus the cloud index for five different classes of sun height. The points represent the average value of the cloud index within a bin (width of the bin : 0.05), the line represents the corresponding linear regression. The variation of the regression coefficients with sun height is given on the first graph.

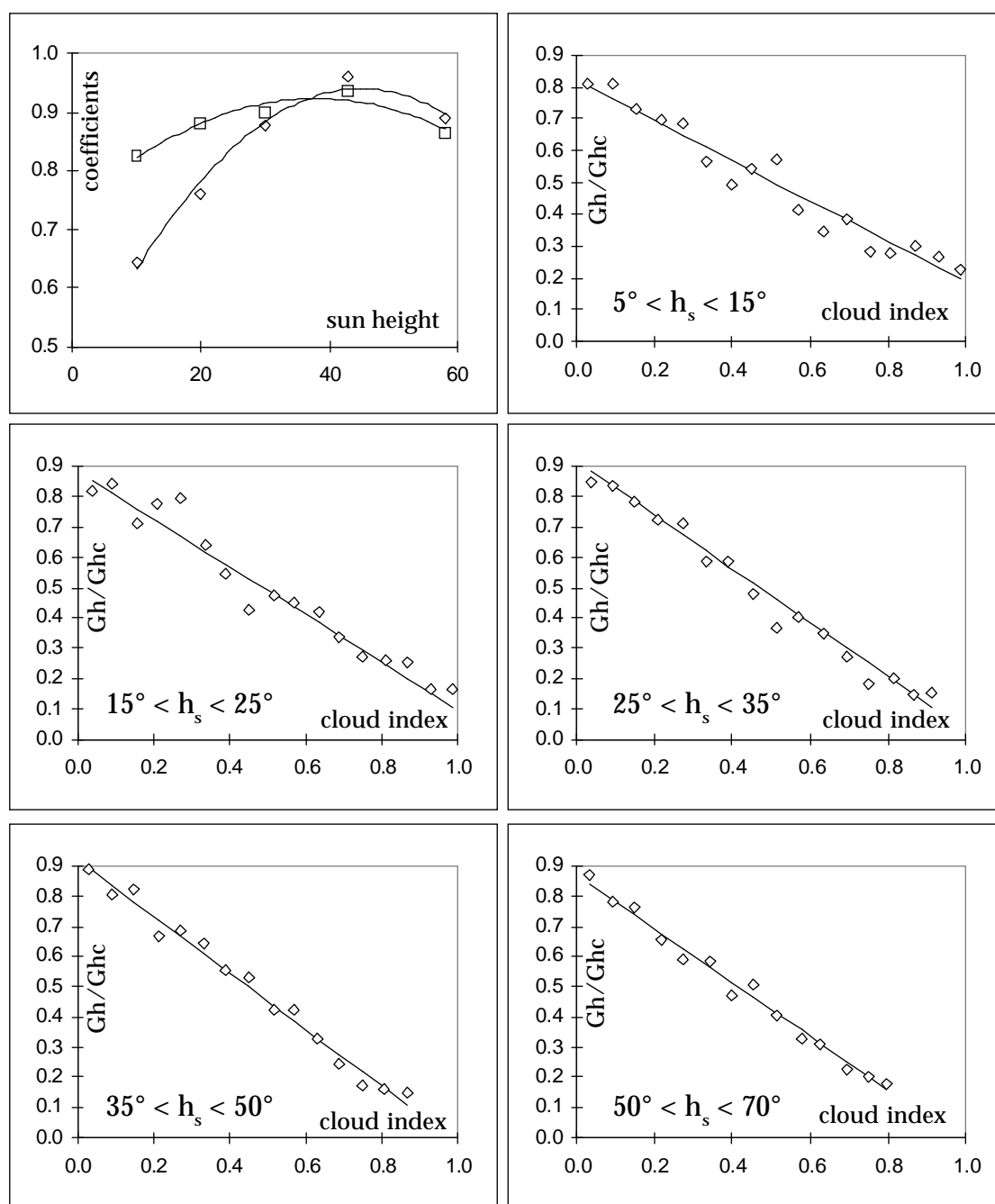


**Figure 3**

Diffuse radiation model derivation.

The second to 6th graphs represent the normalised diffuse versus the cloud index for five different classes of sun height. The points represent the average value of the cloud index within a bin (width of the bin : 0.05), the thick curve represents the corresponding regression, the light curve represents the two parameter model. The variation of the regression coefficients with sun height is given on the first graph.

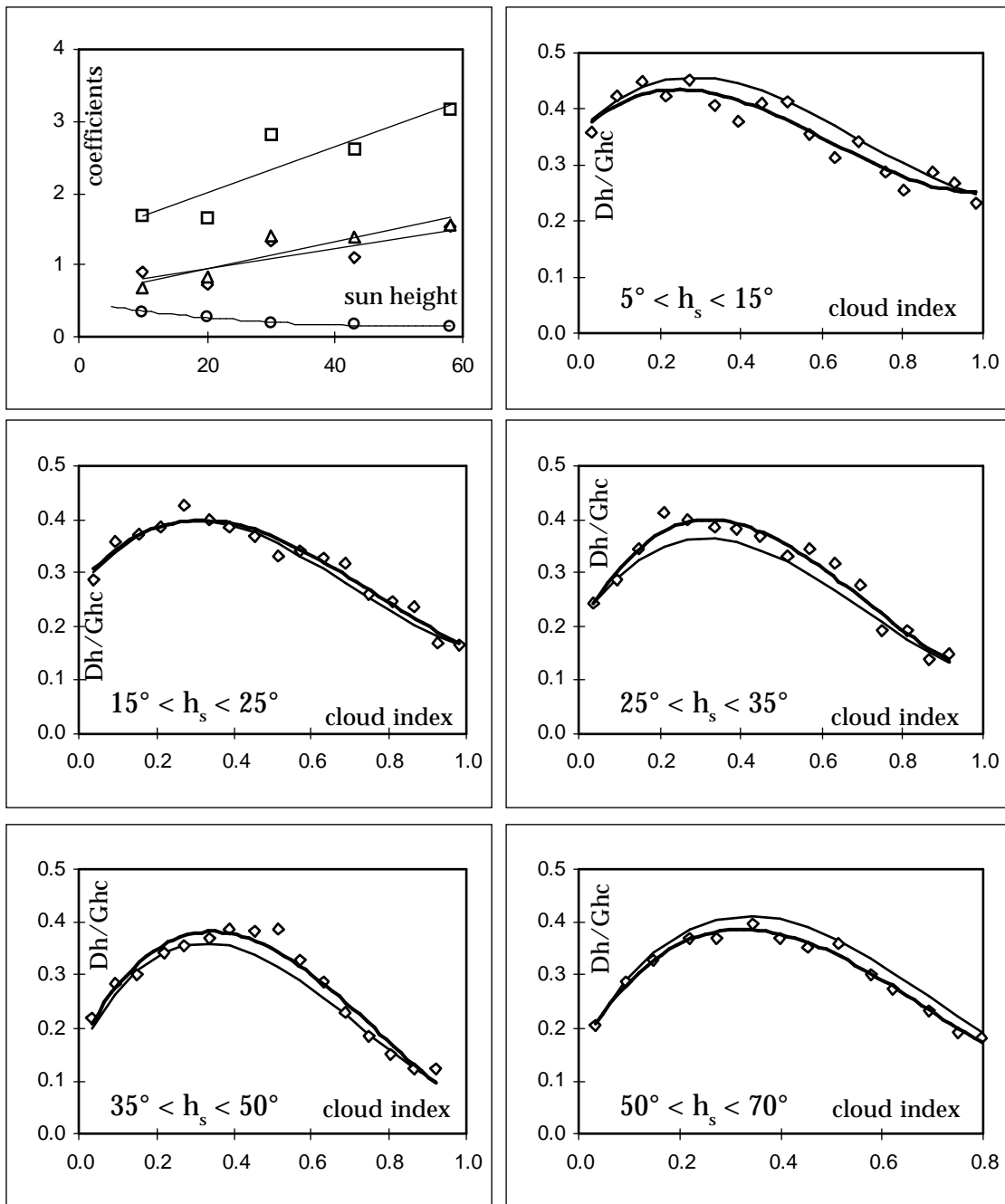


**Figure 4**

Zenith luminance model derivation.

The second to 6th graphs represent the normalised zenith luminance versus the cloud index for five different classes of sun height. The points represent the average value of the cloud index within a bin (width of the bin : .05), the thick curve represents the corresponding regression, the light curve represents the two parameter model. The variation of the regression coefficients with sun height is given on the first graph.

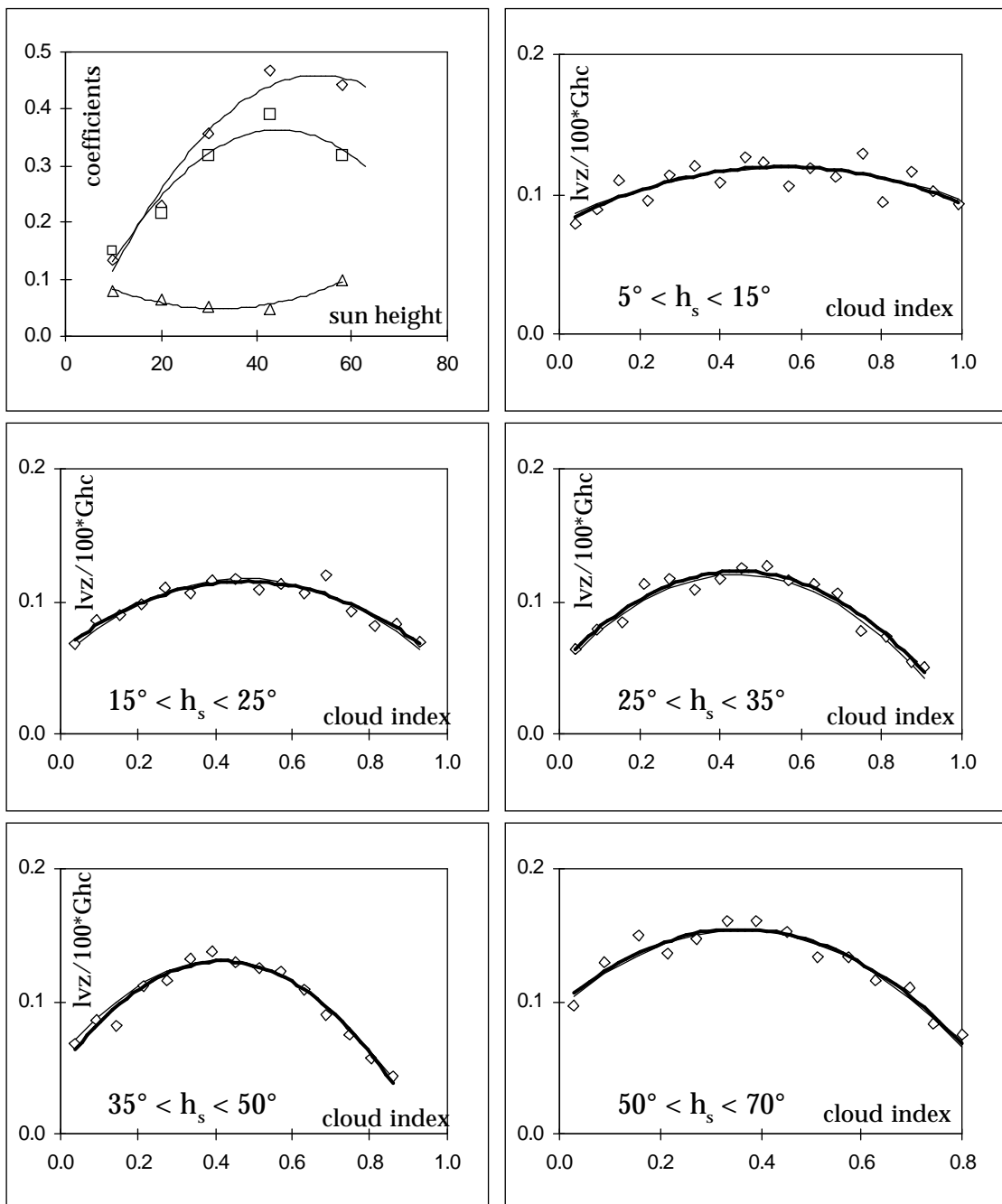
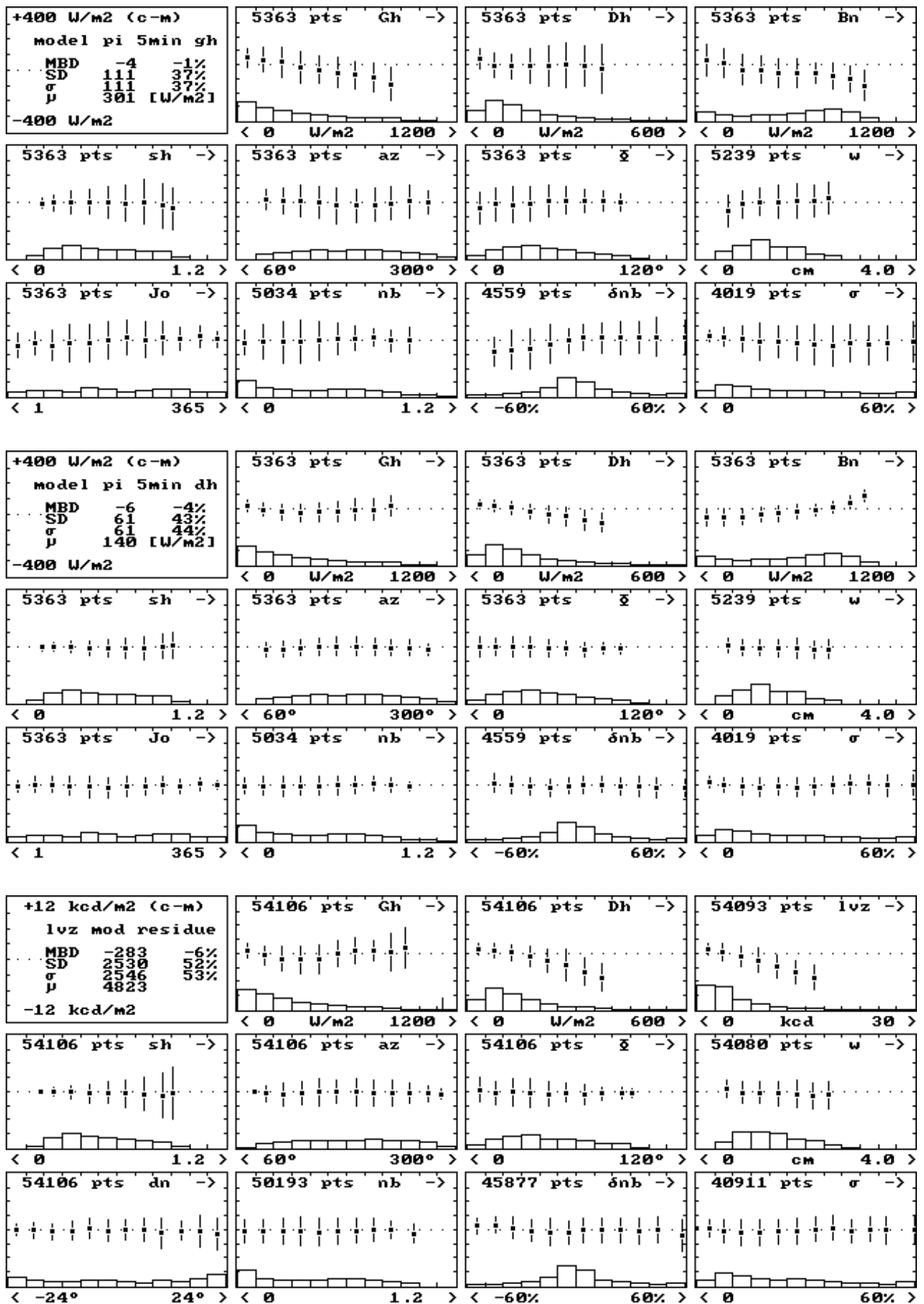
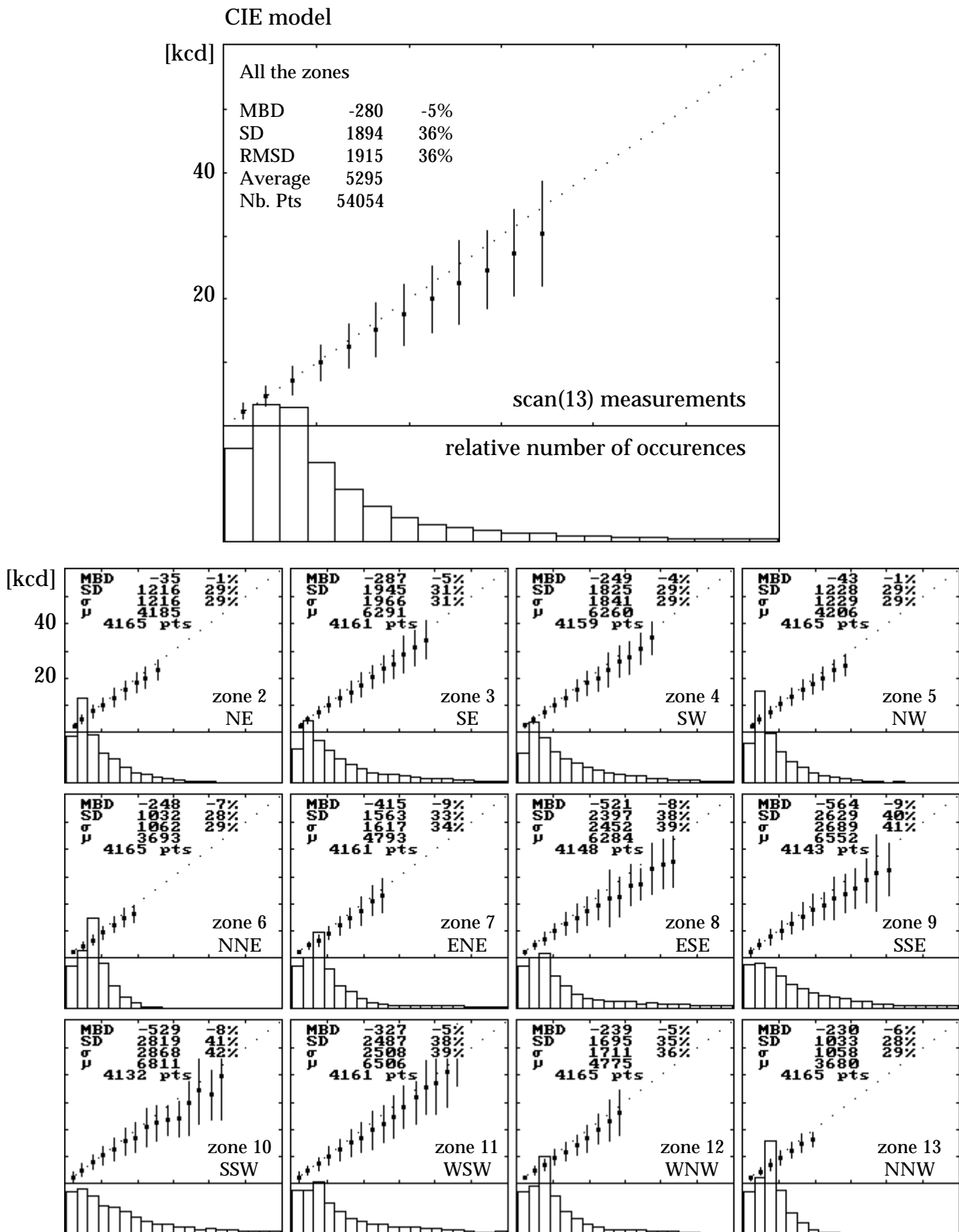


Figure 5 Dependence study for the 3 models (nomenclature & description, see fig 1).



**Figure 6**

Ground based modeled luminance in 13 zones versus corresponding measurement, normalised with the measured diffuse illuminance D<sub>vh</sub>, for all the zones and each zone separately.



**Figure 7**

Pixel based modeled luminance in 13 zones versus corresponding measurement, normalised with the modeled diffuse illuminance Dv<sub>hm</sub>, for all the zones and each zone separately.

CIE model based on a single pixel input

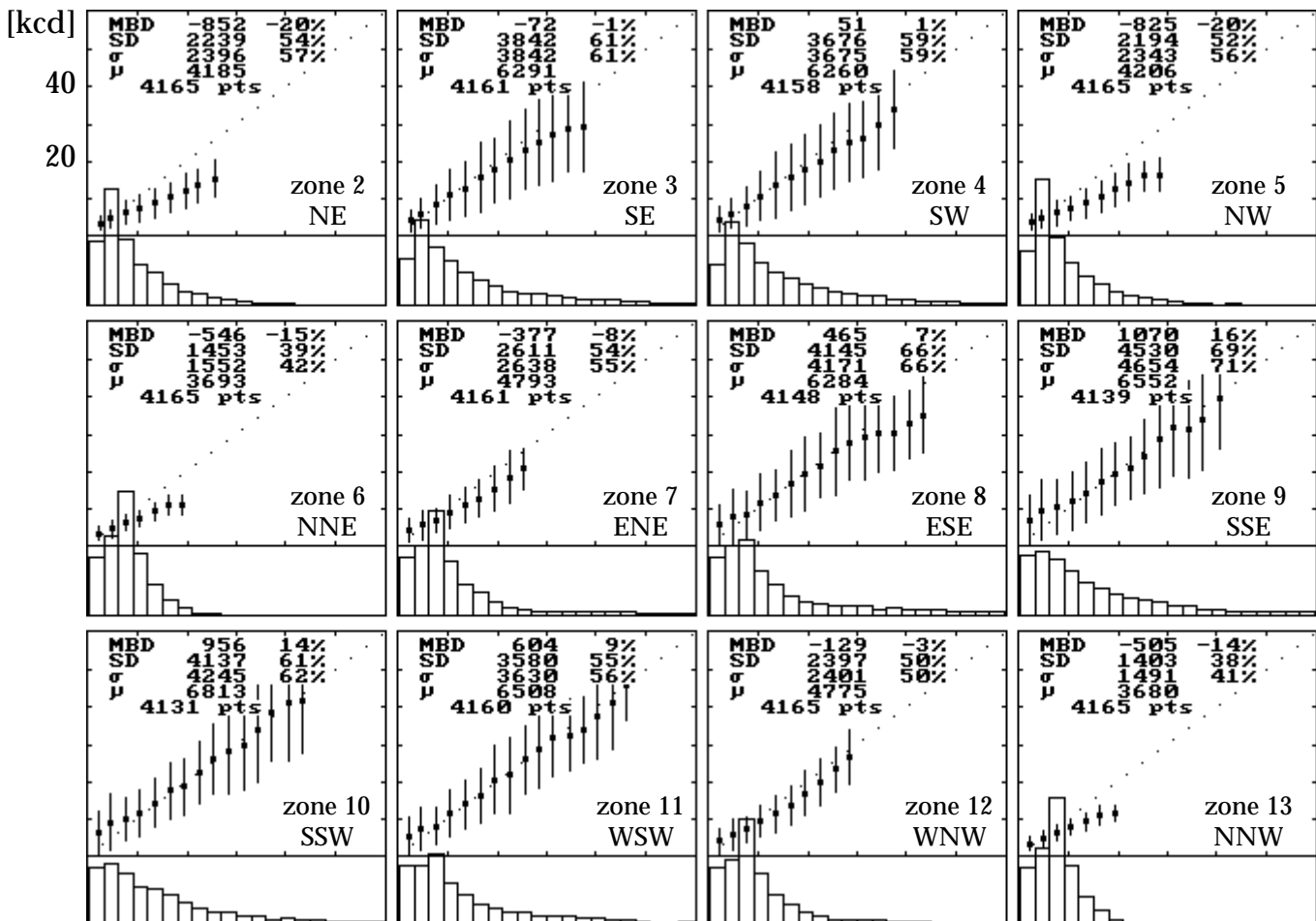
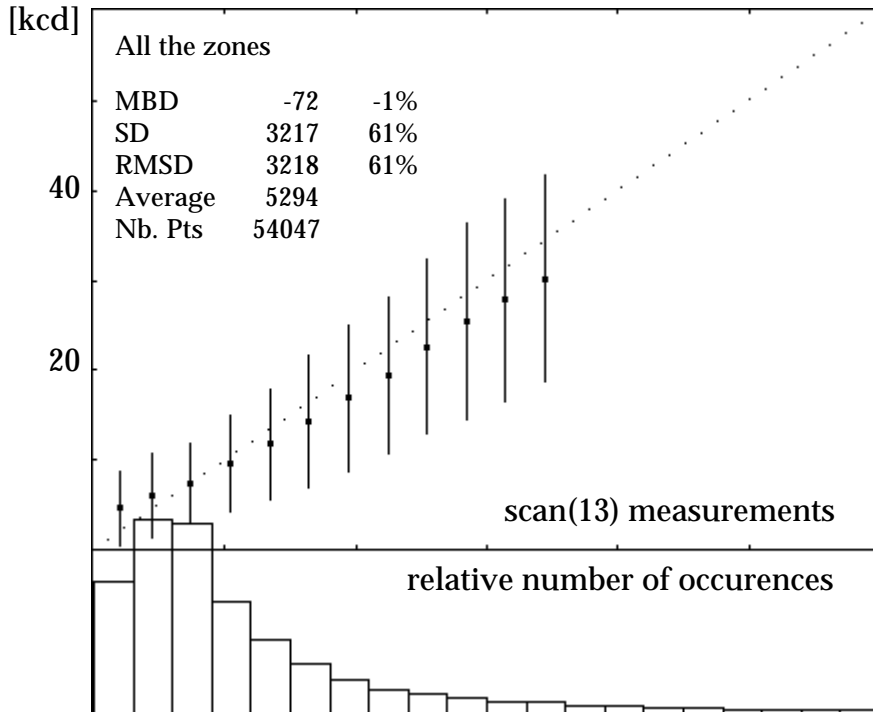


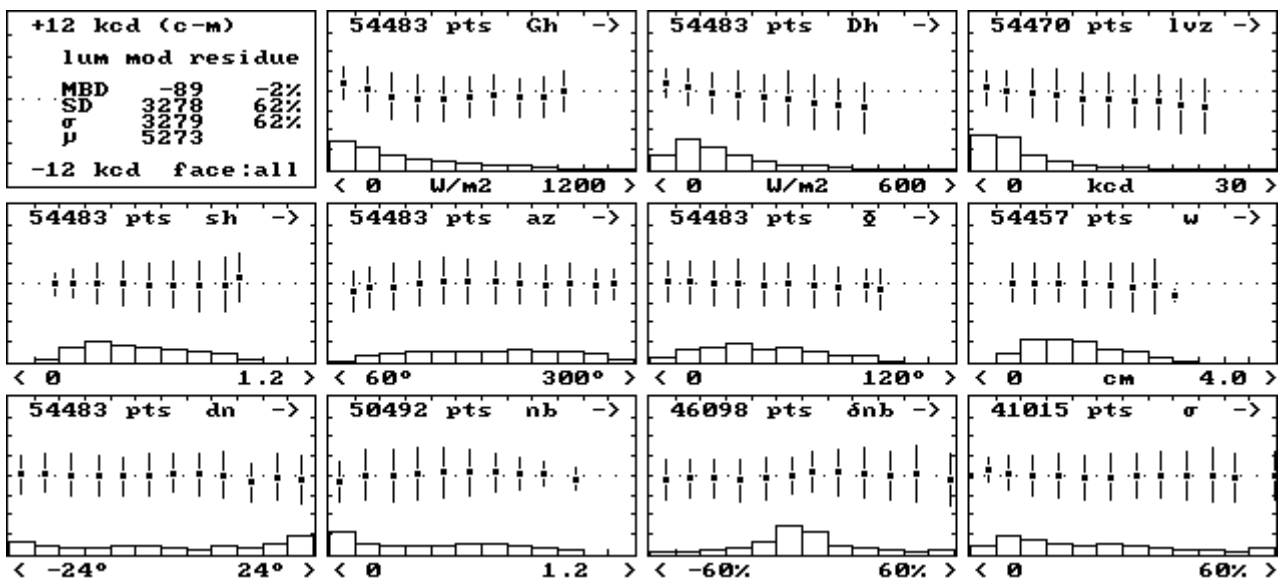
**Figure 8**

Residue of the single pixel luminance model (normalised with the modeled diffuse illuminance  $D_{vhm}$ ), for all 13 zones, the horizon region, and the four vertical directions.

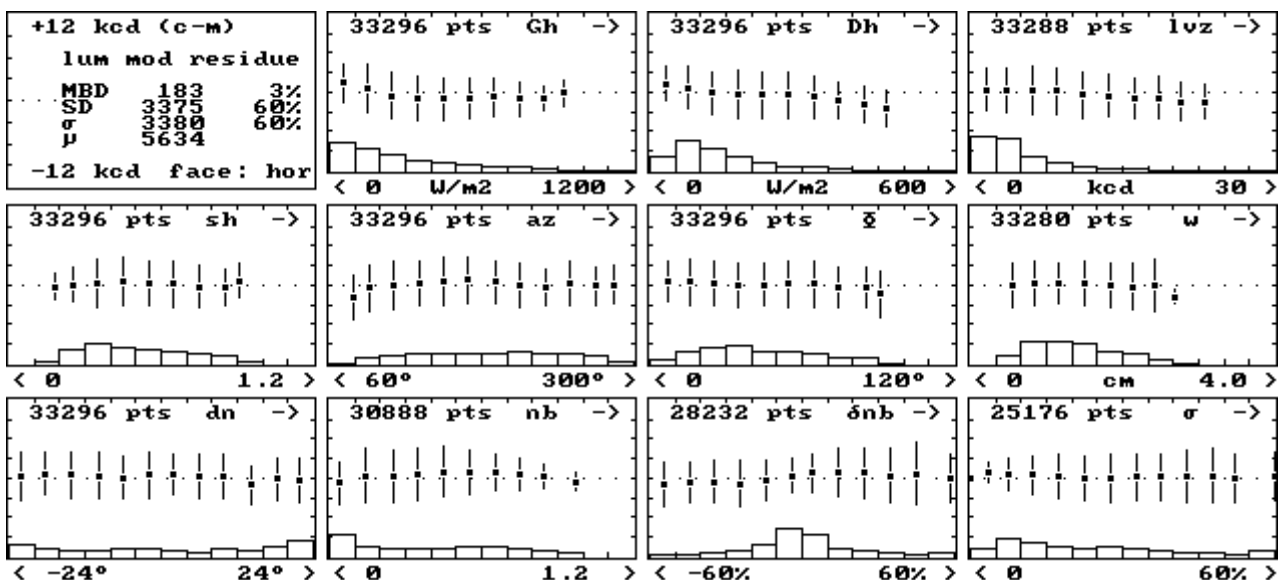
The abscissa scale is divided in bins. For each bin, the mean value is given (point) and is surrounded by  $\pm$  one standard deviation (line). The bar chart at the bottom of each dependence represents the occurrence frequency for each bin in percent of the total number of occurrences. The scale is 20% per graduation.

Gh	horizontal global	sh	sun height sine	Jo	day of the year
Dh	horizontal diffuse	az	sun azimuth	nb	nebulosity index
Bn	normal beam	$\Phi$	sun/satellite angle	$\delta nb$	nb variation (1 pix/15pix)
		w	water vapor	$\sigma$	rmsd (1 pix/15pix)

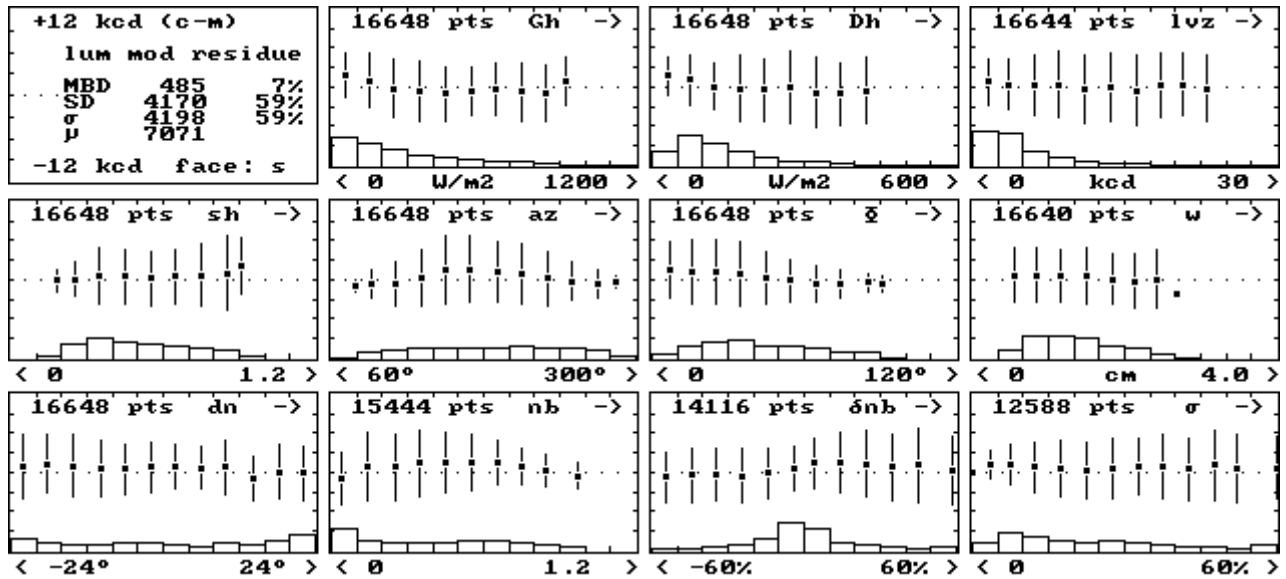
All 13 zones



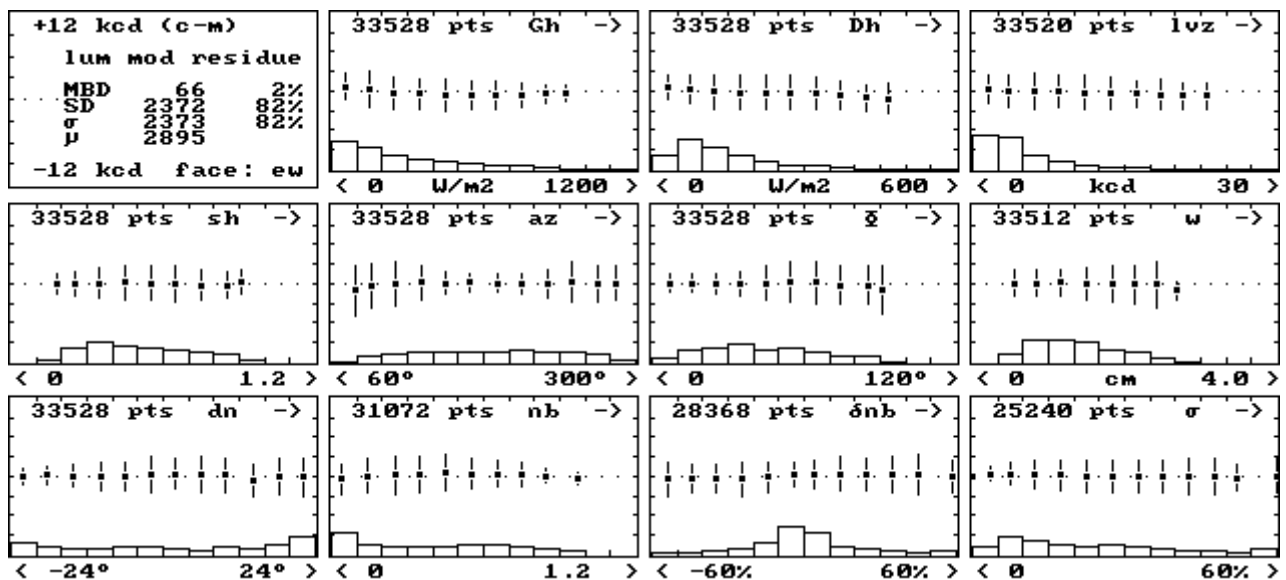
horizon zone (zones 6 to 13)



south (zones 3-4, 9-10)



east-west (zones 2-3, 7-8, 4-5, 11-12)



north (zones 2, 5, 6, 13)

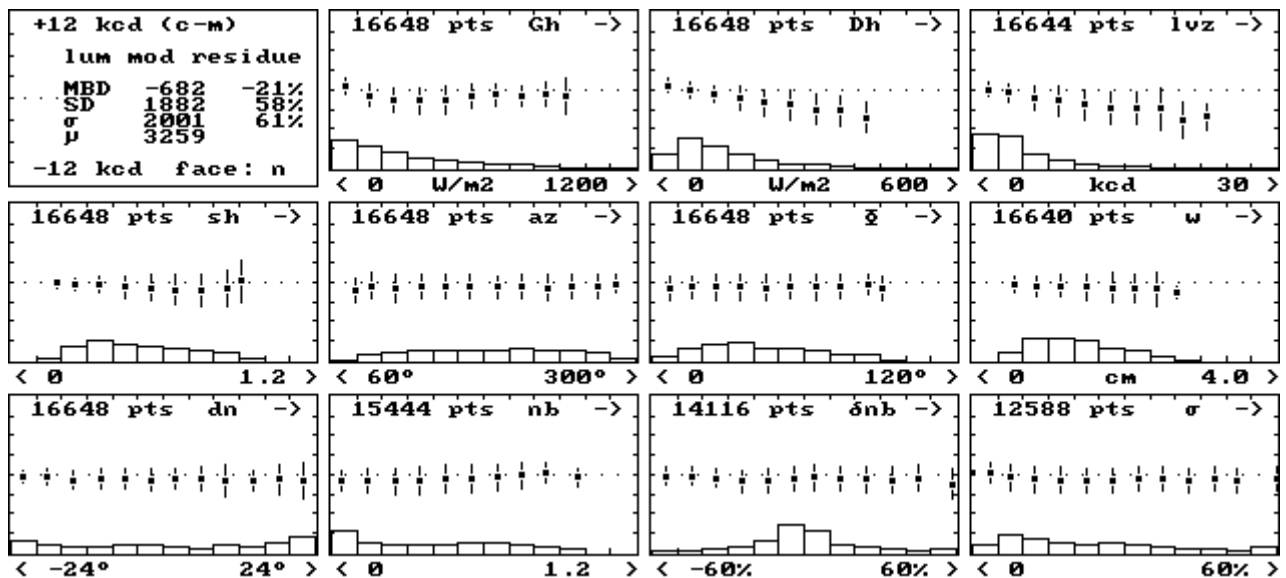


**Figure 9**

Comparison between scan integrals over 6/13 zones, integrals over 72/145 zones and illuminances on vertical planes for measurements.

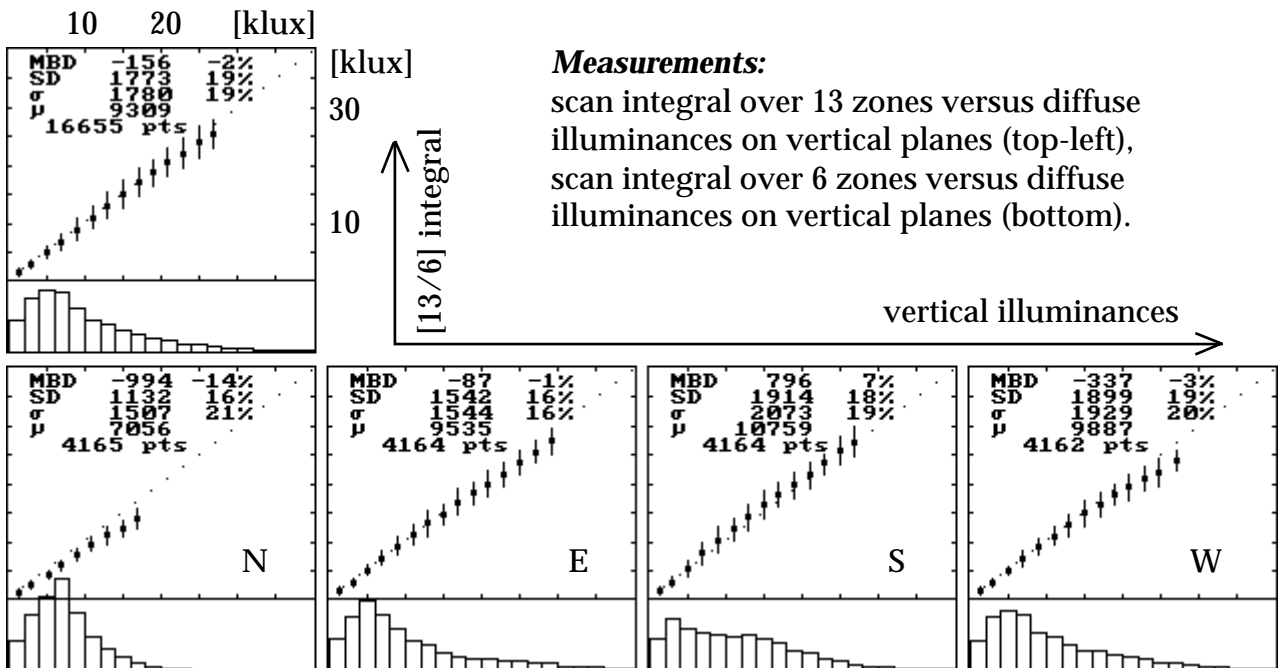
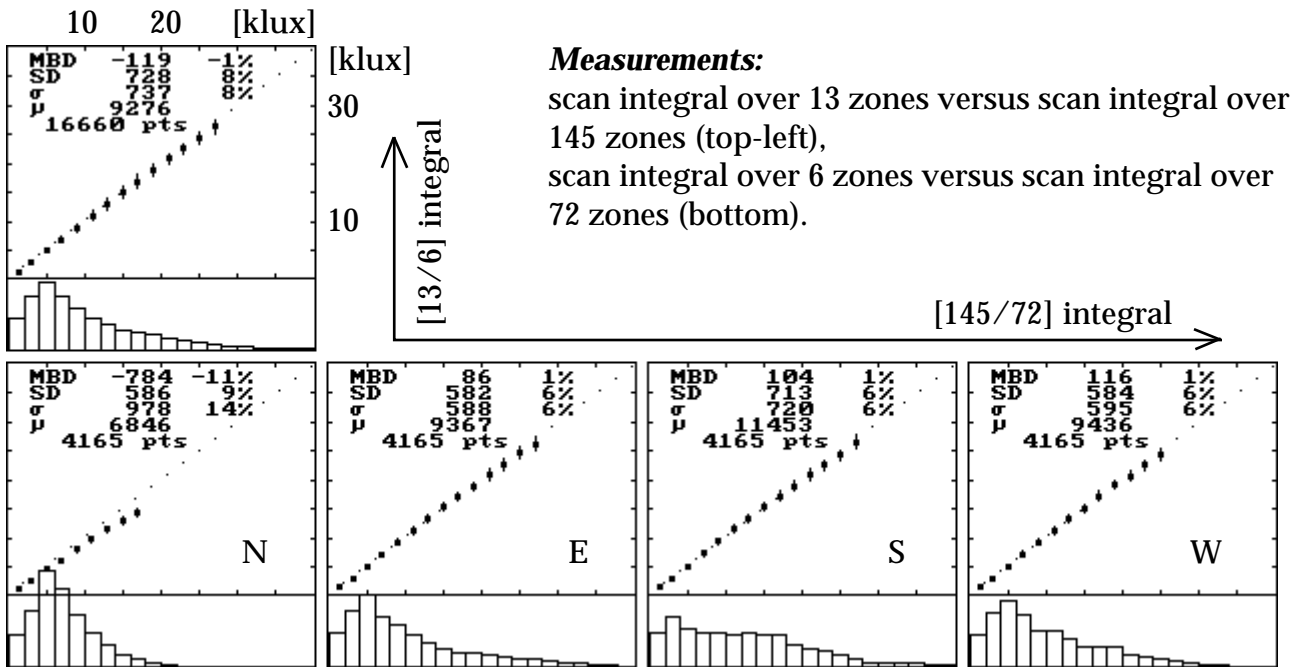


**Figure 10**

Comparison between scan integrals over 6/13 zones and illuminances on vertical planes for CIE/pix2lum model (single pixel model).

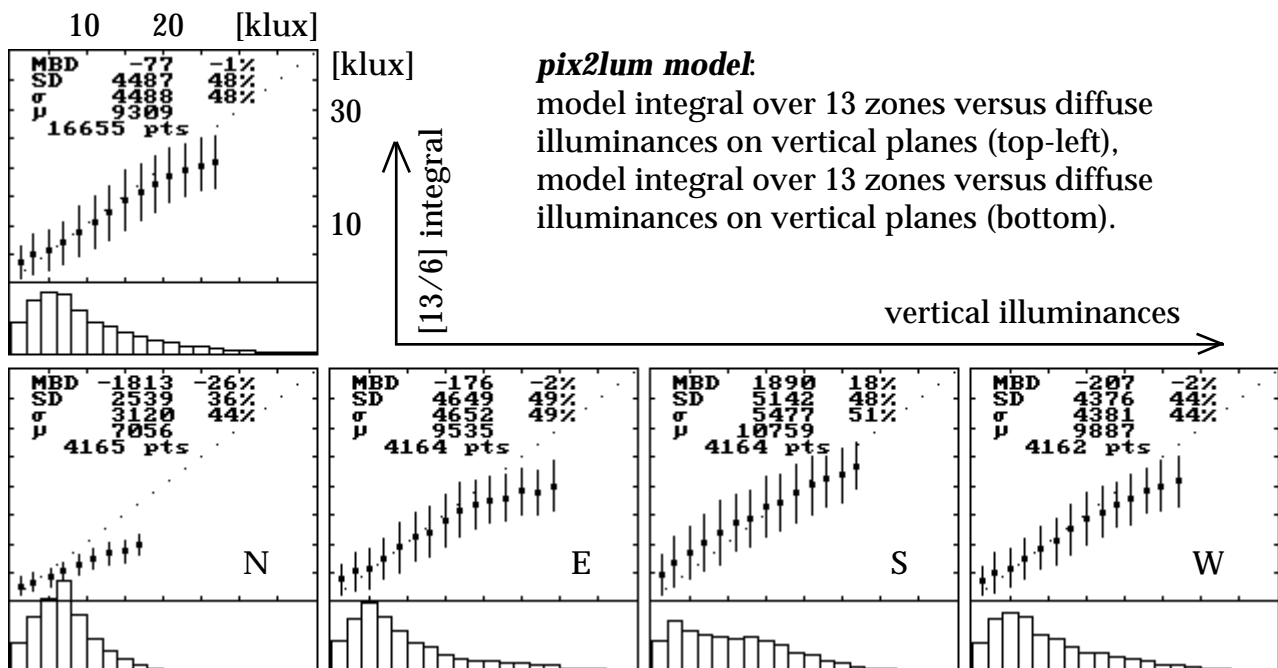
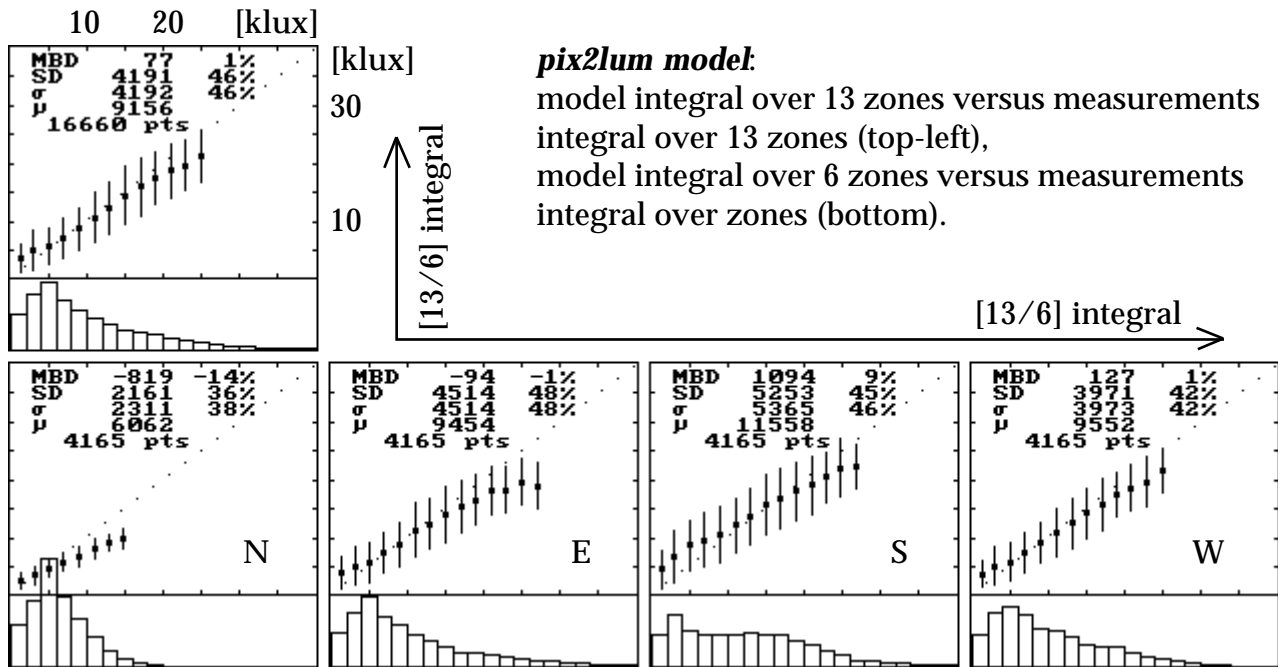


**Figure 11**

Comparison between scan integrals over 6/13 zones and illuminances on vertical planes for CIE ground based model.

